



Experimental study on mechanical damage characteristics of water-bearing tar-rich coal under microwave radiation

Pan Yang · Pengfei Shan · Huicong Xu ·
Jiageng Chen · Zhiyong Li · Haoqiang Sun

Received: 14 June 2023 / Accepted: 14 December 2023
© The Author(s) 2023

Abstract As a recognized special resource, tar-rich coal can extract the country's scarce oil and gas resources and generate semi-coke that can replace anthracite and coking coal. The tar-rich coal in northern Shaanxi is prominent, but due to the dense structure and high strength of tar-rich coal, it is easy to cause frequent dynamic disasters in coal mining. Therefore, the realization of pressure relief and disaster reduction has become the primary problem in mining tar-rich coal. There are many shortcomings in conventional pressure relief methods, so a new

method of microwave-weakening coal is proposed. Through different water saturation treatments of tar-rich coal samples, the longitudinal wave velocity degradation trend and surface crack expansion law of water-bearing coal after microwave irradiation were analyzed, and the strength softening characterization and energy evolution relationship under the combined action of microwave and water were studied. Fractal dimension and its internal correlation based on the equivalent side length-mass of coal sample fragments. The experimental results show that: (1) Under the same microwave radiation condition, with the increase of water saturation, the deterioration trend of physical and mechanical parameters such as longitudinal wave velocity and peak strength is obvious. (2) After microwave radiation, the uniaxial compression results show that the coal sample is damaged by load, there is still a high residual strength, the ratio of elastic energy to dissipation energy decreases, and the possibility of rockburst of the coal sample decreases. The strength softening degree of coal specimen under the degradation of microwave and water is the highest, followed by microwave and water. (3) The fractal dimension is inversely proportional to the moisture content and microwave radiation intensity, and the fractal dimension has a significant positive correlation with the peak intensity and longitudinal wave velocity. The mechanical damage law of water-bearing tar-rich coal under microwave action is revealed, which aims to solve the problem of weakening and reducing the impact of hard coal on-site to a

P. Yang · P. Shan (✉) · H. Sun
College of Energy Science and Engineering, Xi'an
University of Science and Technology, Xi'an 710054,
Shaanxi, China
e-mail: shanpengfei@xust.edu.cn

P. Shan
State Key Laboratory of Coal Resources in Western
China, Xi'an University of Science and Technology,
Xi'an 710054, Shaanxi, China

P. Shan
Key Laboratory of Western Mine Exploration and Hazard
Prevention, Ministry of Education, Xi'an University
of Science and Technology, Xi'an 710054, Shaanxi, China

H. Xu
Department of Civil and Environmental Engineering,
University of Strathclyde, Glasgow G1 1XJ, UK

J. Chen · Z. Li
Xiaojihan Coal Mine, Shaanxi Huadian Yuheng Coal
and Electricity Co., Ltd., Yulin 719000, Shaanxi, China

certain extent, ensure the safety of working face, and improve the mining efficiency of tar-rich coal. It provides basic theoretical support for microwave-assisted hydraulic fracturing technology and effective weakening measures for hard roof treatment.

Article Highlights

1. Study the damage difference of coal samples under the dual factors of microwave power and moisture content.
2. Qualitatively analyzed the crack evolution rules of oil-rich coal samples with different moisture contents under microwave radiation.
3. Explored the effect of microwave-water interaction on the sensitivity of mechanical parameters of coal samples.

Keywords Microwave radiation · Moisture content · Tar-rich coal · Energy evolution · Crack expansion · Fractal dimension

1 Introduction

As a recognized special resource, tar-rich coal can extract the country's scarce oil and gas resources, generate semi-coke that can replace anthracite and coking coal, and has the advantages of high oil and gas conversion efficiency and low production cost (Ju et al. 2021). The coal in northern Shaanxi is rich in oil, and the amount of tar-rich coal resources is more than 150 billion tons, ranking first in the country. Among them, the tar yield of Triassic tar-rich coal in northern Shaanxi is as high as 11.75% on average, and about 0.76 tons of clean oil can be produced per ton of tar, which has great development potential (Shi et al. 2023). However, due to the dense structure and high strength of tar-rich coal, there are some problems in the mining process, such as large mining thickness, large roadway section, the large strike length of the working face, and fast advancing speed (Zhang et al. 2016). As a result, the problem of dynamic disasters in coal mining is frequent, so the realization of pressure relief and disaster reduction has become the primary problem in the mining of tar-rich coal. However, conventional pressure relief methods (hydraulic fracturing (Gu et al. 2015;

Khadijeh et al. 2022), blasting pressure relief (Luo et al. 2021), and large-diameter drilling pressure relief (Zhang et al. 2019), etc.) have problems such as poor orientation, easy derivation of other disasters, and low efficiency. Therefore, this paper proposes a new method of microwave weakening coal (Li et al. 2020), which aims to solve the problem of weakening and reducing hard coal on-site to a certain extent, ensure the safety of the working face, and improve the efficiency of tar-rich coal mining.

Compared with traditional pressure relief technology, microwave radiation has the following advantages: clean, low cost, and good orientation (Yang et al. 2021; Mushtaq et al. 2014). In recent years, the effect of microwave radiation on coal is remarkable, and the research form and content are increasing day by day. In the field of microwave radiation of rock mass, microwave radiation can cause cracking of shale matrix. Cracks are first formed in quartz grains, which are caused by uneven heating caused by the difference of intermediate electrical constants of mineral components. (Liu et al. 2022). As a high dielectric constant mineral, basalt contains more Si, Fe, and Al elements (Zhang et al. 2022). Under the condition of triaxial anisotropic stress, the basalt specimen produces a fracture network dominated by tensile cracks after microwave drilling and fracturing, which reduces the energy and stress concentration in the rock mass and achieves the effect of preventing deep hard rock rockburst (Deyab et al. 2020). At the same time, the process of microwave pyrolysis of basalt is intermittent (quiet-active-quiet), the cracks are continuously developed, and the crack width is suppressed (Feng et al. 2021). The microwave sensitivity of sandstone is low, and the main reason for microwave crushing of water-bearing sandstone is the stress change caused by water vapor expansion and mineral thermal expansion (Lu et al. 2022). The effective ways to crack sandstone are high microwave power, low air fluidity, and high water saturation. (Zhao et al. 2020). The biotite in the granite component is a high-absorbing mineral, which produces thermal stress difference from other weak-absorbing minerals, resulting in rock cracking and fracture toughness reduction (Bai et al. 2021; Nicco et al. 2020). In the process of deep resource drilling, the stress around the granite reservoir is redistributed under the interaction of ground stress

and thermal stress, forming a disturbance degradation zone and a disturbance pressure relief zone (Xu et al. 2022). According to the distribution of micro-cracks and macro-cracks of diorite, the microwave damage zone is divided into a broken zone, fracture zone, and discrete debris zone (Ma et al. 2022). The best microwave radiation power for gabbro is 3.3kw, and the failure mode of specimens is mainly tensile shear failure in the vertical direction (Ge and Sun 2021). In addition, microwave power, treatment time and mineral composition will significantly affect the heating degree of magmatic rocks (Kahraman et al. 2020). In the field of microwave radiation of coal, the microwave is heated in the form of a coal sample as a whole, and the temperature and stress are concentrated. The internal of the coal sample is dominated by compressive stress failure, and the external edge of the coal sample is dominated by tensile stress failure (Zhang et al. 2022). After microwave irradiation, wave velocity and other physical and mechanical parameters of the specimen in different directions deteriorated to different degrees. (Hong et al. 2020). Microwave selective heating causes the uneven thermal distribution of coal, resulting in a temperature gradient and high thermal stress. When the temperature exceeds a certain limit, the microcracks expand and extend (Zhang et al. 2017; Ellison et al. 2022). The dominant transformation effect of microwave on the pore structure of coal samples is open pore and sparse pore (Li et al. 2017). After microwave cracking of coal samples, the post-peak softening modulus decreases, which increases the critical load of rock burst in the roadway, thus reducing the possibility of rock burst (Hu et al. 2021). As a high dielectric constant material, bound water and free water in minerals will dissipate during microwave radiation, and the dissipation of water will greatly change the heating characteristics of minerals (Hu et al. 2020).

The existing research rarely involves the fracture development and weakening transformation of tar-rich coal under the combined action of moisture

content and microwave. Given this, in this paper, the tar-rich coal was treated with different water saturation and the longitudinal wave velocity degradation trend and surface crack expansion law of the water-bearing coal body after microwave irradiation were analyzed. The strength softening characterization, energy evolution relationship, and fractal dimension based on the equivalent side length-mass of coal sample fragments and their internal correlation were studied. The mechanical damage law of water-bearing tar-rich coal under microwave action is revealed, Provides basic theoretical support for microwave-assisted hydraulic fracturing technology, and Provides effective weakening measures for hard roof control.

2 Experimental design

2.1 coal sample preparation

The tar-rich coal specimens were taken from the Xiaojihan Coal Mine in Yuyang District, Yulin City, Shaanxi Province. All coal samples were taken from the whole coal body so that the anisotropy of the coal was minimized. The selected coal samples were drilled by the drilling machine, and the smoothness was guaranteed by the equal operation of the profiler and the grinding machine. The samples were processed into cylindrical specimens with a diameter of 50 mm and a height of 100 mm. The component analysis of the coal samples was shown in Table 1.

2.2 experimental scheme

The experimental equipment is a self-developed microwave radiation experimental device with a microwave frequency band of 2450 MHz and a maximum microwave power of 2.0 kW. The RMT-150B rock mechanics test system (loading control system) and RSM-SY5 (T) nonmetallic acoustic wave detector are designed by the Wuhan Institute of Rock

Table 1 Test piece component analysis table

Coal sample type	Tar yield (%)	Industrial ingredients (%)				Elementary composition (%)			
		Fixed carbon	Moisture	Ash	Volatile	C _{daf}	H _{daf}	N _{daf}	O _{daf}
Tar-rich coal	8.17	58.13	4.12	4.68	33.06	82.11	4.46	0.79	12.63

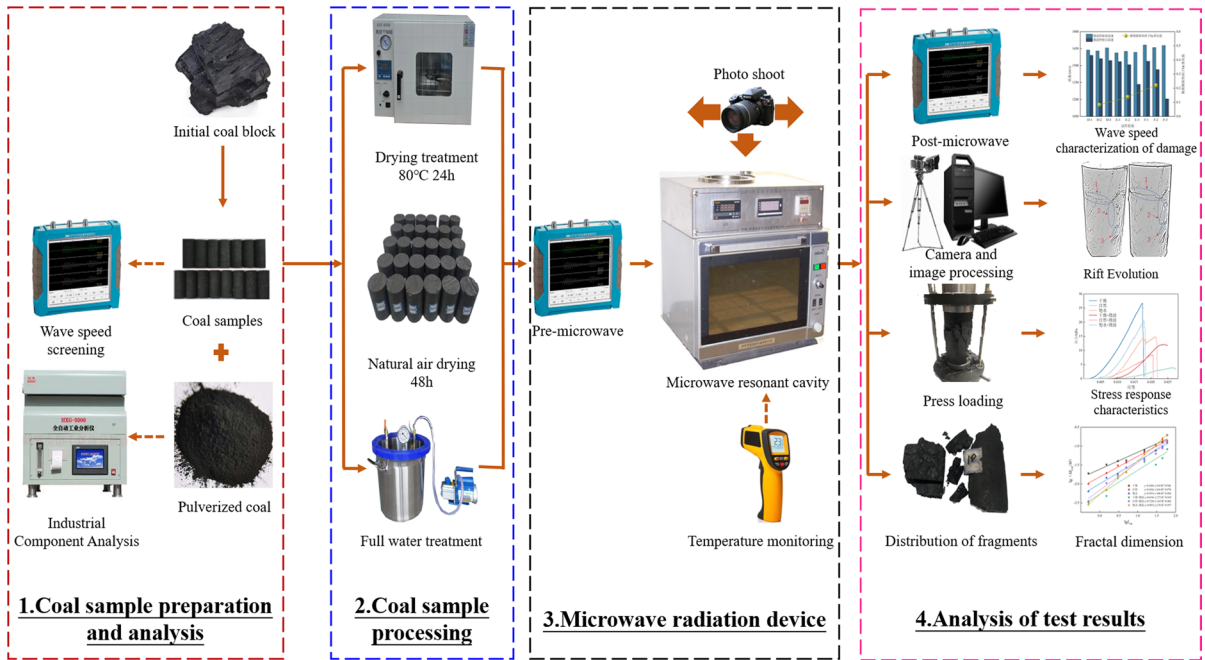


Fig. 1 Test flow

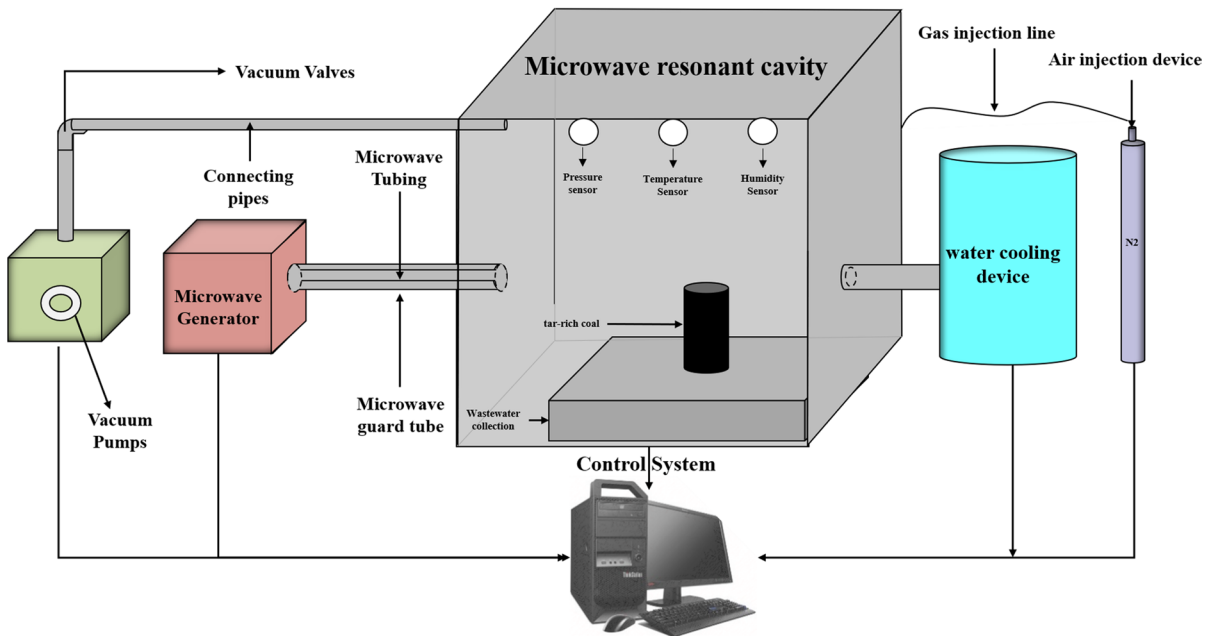


Fig. 2 Schematic diagram of the microwave radiation system

Table 2 Microwave radiation test scheme

Specimen number	Sample treatment method	Microwave power (P/KW)	Single radiation time (t/s)
A _{1,2,3}	Dry heat treatment	0	0
B _{1,2,3}	Natural air drying	0	0
C _{1,2,3}	Saturated water treatment	0	0
D _{1,2,3}	Dry heat treatment	2	60
E _{1,2,3}	Natural air drying	2	60
F _{1,2,3}	Saturated water treatment	2	60
G _{1,2,3}	Dry heat treatment	0.5	120
G _{4,5,6}	Dry heat treatment	1	120
G _{7,8,9}	Dry heat treatment	2	120
H _{1,2,3}	Natural air drying	0.5	120
H _{4,5,6}	Natural air drying	1	120
H _{7,8,9}	Natural air drying	2	120
I _{1,2,3}	Saturated water treatment	0.5	120
I _{4,5,6}	Saturated water treatment	1	120
I _{7,8,9}	Saturated water treatment	2	120

and Soil Mechanics, Chinese Academy of Sciences. The experimental process is shown in Fig. 1, and the microwave radiation system is shown in Fig. 2.

As shown in Table 2, all coal samples were labeled and treated with different water saturation. The specimens were divided into natural groups, dry groups, and saturated groups according to their composition. The test was divided into 9 groups. Group A, B, and C were pressure-loading groups. The peak strength and physical and mechanical parameters of the specimens under different water saturation were analyzed. Groups D, E, and F were microwave irradiation + press loading groups. Under different moisture contents, the same microwave power (2KW) was irradiated for the same time (60 s). Groups H, I, and G were microwave irradiation + uniaxial compression group, and at the same time (120 s) was irradiated at different microwave irradiation powers (0.5KW,1KW,2KW). The changes in mechanical parameters of coal samples under different water contents were measured in groups A, B, and C. The changes in longitudinal wave velocity and mechanical parameters of coal samples before and after

microwave irradiation under the same microwave parameters and different water contents were measured in groups D, E, and F. The changes in longitudinal wave velocity and mechanical parameters of coal samples before and after microwave irradiation under the same water content, the same microwave irradiation time, and different microwave irradiation power were investigated. Group G was the change of physical and mechanical parameters of dry samples before and after microwave irradiation. The influence of moisture content and microwave irradiation parameters on coal sample specimens was studied separately, and the interaction between the two factors was studied.

The test steps are as follows:

1. Put the prepared dry group coal sample into the vacuum drying oven, and dry at 80 °C for 24 h, through weighing measurement, it is considered that the moisture content is 0. After the temperature was lowered to room temperature, the longitudinal wave velocity before microwave irradiation was measured by an ultrasonic detector. The prepared natural water-bearing group coal sample specimens were air-dried for 48 h. Through weighing measurement, it was considered that the water content was the same in this state (the water content of the natural group was 3.24%, and the water content of the natural and microwave group was 3.17%). The longitudinal wave velocity of the natural group coal sample was measured by ultrasonic before microwave irradiation. The free immersion method was used to prepare the saturated water-bearing group coal sample. Through weighing measurement, it was considered that the water content was the same in this state (the water content of the saturated group was 5.57%, and the water content of the saturated and microwave group was 5.61%). The ultrasonic detector was used to measure the longitudinal wave velocity of the saturated group coal sample before microwave irradiation.
2. Put the coal sample into the microwave resonant cavity, open the gas injection equipment, inject N₂ into the microwave resonant cavity, discharge the excess oxygen in the cavity, and then seal the operation, continue to inject N₂, so that the internal environment is close to the anaerobic

environment, to avoid spontaneous combustion of coal samples.

3. The microwave generator is turned on, and the microwave energy enters the microwave resonant cavity through the waveguide tube, acting on the coal sample specimen, so that the temperature is increased, and the higher content of tar and other substances is infiltrated to form cracks.
4. When the predetermined microwave irradiation parameters are reached, the microwave resonant cavity stops working, the coal sample specimens are taken out, and the surface temperature and fracture network development are recorded.
5. After falling to room temperature, the longitudinal wave velocity of the specimen after microwave irradiation was measured by an ultrasonic detector.
6. Before the loading of the press, a rubber gasket is added to the contact surface of the coal sample to minimize the influence of the end effect. The rock mechanics loading control system is used to perform uniaxial loading tests on all coal sample specimens.
7. After the test, record the test data and analyze the test results.

3 Experiment results

3.1 Macro-scale fracture evolution law

3.1.1 Damage difference of coal samples under two factors of microwave power and water content

The damage definition methods mainly include defining the damage varies according to the pore area, defining the damage tensor, and characterizing the internal damage degree of the coal specimen according to the macroscopic changes such as Young's modulus and ultrasonic wave velocity (Zhao et al. 2016; Gautam et al. 2016). In these three definition methods, macroscopic variables such as ultrasonic wave velocity are the most convenient to characterize the internal damage degree of coal sample specimens. The ultrasonic wave velocity is mainly affected by the development of internal cracks in coal specimens. The denser the specimen is, the greater the wave velocity is. On the contrary, the more developed the internal cracks in the specimen are, the smaller the wave velocity is.

The ultrasonic wave velocity of the coal sample is measured in the vertical direction of the cylindrical coal sample, and the longitudinal wave velocity can be expressed as:

$$V = \frac{L}{\Delta t} \quad (1)$$

In the formula, V is the ultrasonic wave velocity, $\Delta t = t_2 - t_1$, t_1 is the time when the probe on the ultrasonic detector emits the ultrasonic wave, and t_2 is the time when the lower probe receives the ultrasonic wave.

Table 3 Changes of wave velocity and elastic modulus of coal samples with different water contents before and after microwave irradiation

Specimen number	Pro-microwave (m/s)	Post-microwave (m/s)	Specimen number	Pro-microwave (m/s)	Post-microwave (m/s)
A _{1,2,3}	1693.9	–	G _{7,8,9}	1632.6	1479.3
B _{1,2,3}	1719.2	–	H _{1,2,3}	1618.2	1557.8
C _{1,2,3}	1806.6	–	H _{4,5,6}	1623.7	1508.6
D _{1,2,3}	1649.7	1539.6	H _{7,8,9}	1617.5	1306.7
E _{1,2,3}	1622.8	1313.5	I _{1,2,3}	1606.9	1553.8
F _{1,2,3}	1677.8	1205.3	I _{4,5,6}	1642.6	1407.5
G _{1,2,3}	1607.4	1519.2	I _{7,8,9}	1679.2	1207.3
G _{4,5,6}	1619.7	1559.3	–	–	–

The ultrasonic wave velocity of coal samples can indirectly reflect the development of internal micro-cracks. According to the research results of existing scholars (Lin and Chen 2005; Tripathi et al. 2021), the quantitative characterization of the internal crack development of coal samples under microwave irradiation is:

$$D_c = 1 - \left(\frac{V_1}{V_0}\right)^2 \tag{2}$$

In the formula, D_c represents the micro-crack damage factor of the coal sample specimen defined by ultrasonic wave after microwave radiation, V_0 is the ultrasonic wave velocity of the coal sample specimen in the initial state without microwave irradiation, m/s, V_1 is the ultrasonic wave velocity of coal sample specimen after microwave irradiation once, m/s. The wave velocity relationship of some coal samples before and after the microwave is shown in Table 3.

Introducing microwave radiation, under the same microwave irradiation time and microwave power, the relationship between ultrasonic wave velocity and microcrack damage factor of coal samples under different water content conditions is studied, thus, the influence of microwave on the development results

of microfissure in coal samples is preliminarily determined when water is involved.

By microwave irradiation group D, E, and F group before and after the vertical direction of the coal sample wave velocity and the change of coal sample D_c microfracture damage factor relations as shown in Fig. 3. The wave velocity measured in the vertical direction of the specimen in the dry state is reduced from 1627.5~1656.7 m/s to 1544.5~1588.6 m/s, with an average decrease of 4.17% and a maximum decrease of 6.82%. Under the condition of natural water content, the wave velocity measured in the vertical direction of the specimen decreased from 1589.3~1629.3 m/s to 1327.3~1517.6 m/s, with an average decrease of 7.16% and a maximum decrease of 17.29%. The wave velocity measured in the vertical direction of the specimen in the saturated state decreased from 1649.5~1679.3 m/s to 1207.6~1459.7 m/s, with an average decrease of 11.63% and a maximum decrease of 28.32%.

Under normal circumstances, the rock mass with the same fracture rate, the water content increases, the internal pores and cracks of the coal sample specimen are filled, and the ultrasonic wave velocity should increase. However, because tar and water molecules belong to substances with high dielectric

Fig. 3 Changes of longitudinal wave velocity and micro-crack damage factor of tar-rich coal under different moisture content before and after the same microwave parameter irradiation

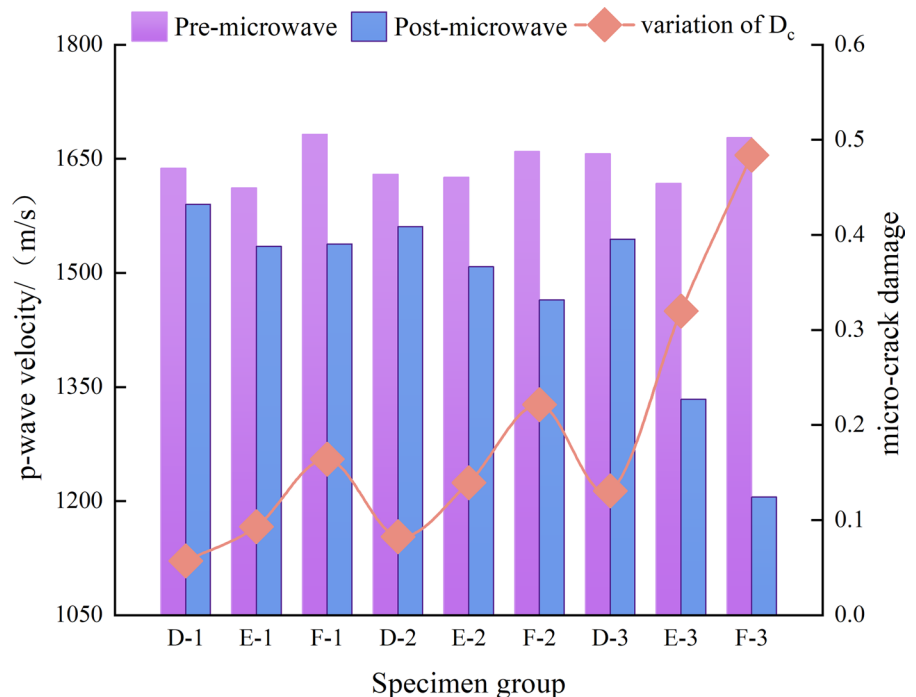
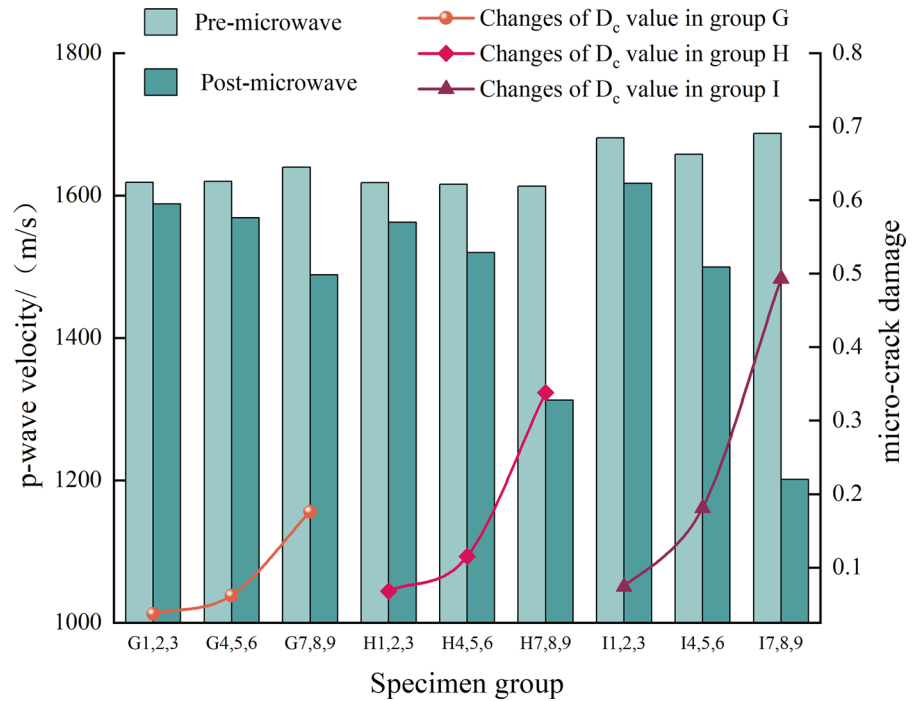


Fig. 4 Under the same microwave irradiation time, before and after applying different microwave power, the changes in longitudinal wave velocity and microcrack damage factor of tar-rich coal in different water-bearing states



constant, with the introduction of microwave, tar, which accounts for a relatively high proportion of the components in tar-rich coal, is pyrolyzed with the increase of temperature. The continuous escape of pyrolysis products makes a large number of pores and cracks generated inside the coal sample. And with the increase of temperature, the water in the original pores and fissures in the interior is vaporized, generating water vapor, and the vapor pressure is generated and acted on the coal sample aperture fissures, forming a similar effect to splitting tensile, making the pores and fissures further expand. On the other hand, the water on the surface of the coal sample evaporates to produce water vapor due to the microwave field environment, which further increases the temperature in the microwave field and promotes the inoculation and expansion of the coal microstructure. Due to these reasons, the moisture content increased making the wave velocity of coal samples far less than water and tar due to the temperature under microwave irradiation micro-crack structure led to the degree of wave velocity decreases. Therefore, the introduction of microwave and the increase of moisture content make the pores and cracks of the coal sample increase, and the trend of ultrasonic wave speed decrease is obvious,

which leads to the deterioration of the coal sample strength.

Figure 4 is the change of longitudinal wave velocity and micro-fracture damage factor in group G, group H and the group I under different microwave radiation intensities. As shown in the figure, under the irradiation of dry state and low microwave power, the development of micro-cracks in coal samples is not obvious. It is because the microwave power is low and the heating effect is not obvious, only less polar substances are volatilized, so that the longitudinal wave velocity is slightly reduced, and the change of micro-crack damage factor is small. With the gradual increase of microwave power, the longitudinal wave velocity of coal samples in different states decreases, and the micro-crack damage factors increase to varying degrees. When the microwave power increases from 1 to 2kw, the surface and internal cracks of coal samples further develop and expand, and the microwave damage factor increases. At the same time, due to the increase of water saturation and microwave radiation energy, it is found that the change of micro-fracture damage factor shows an increasing trend.

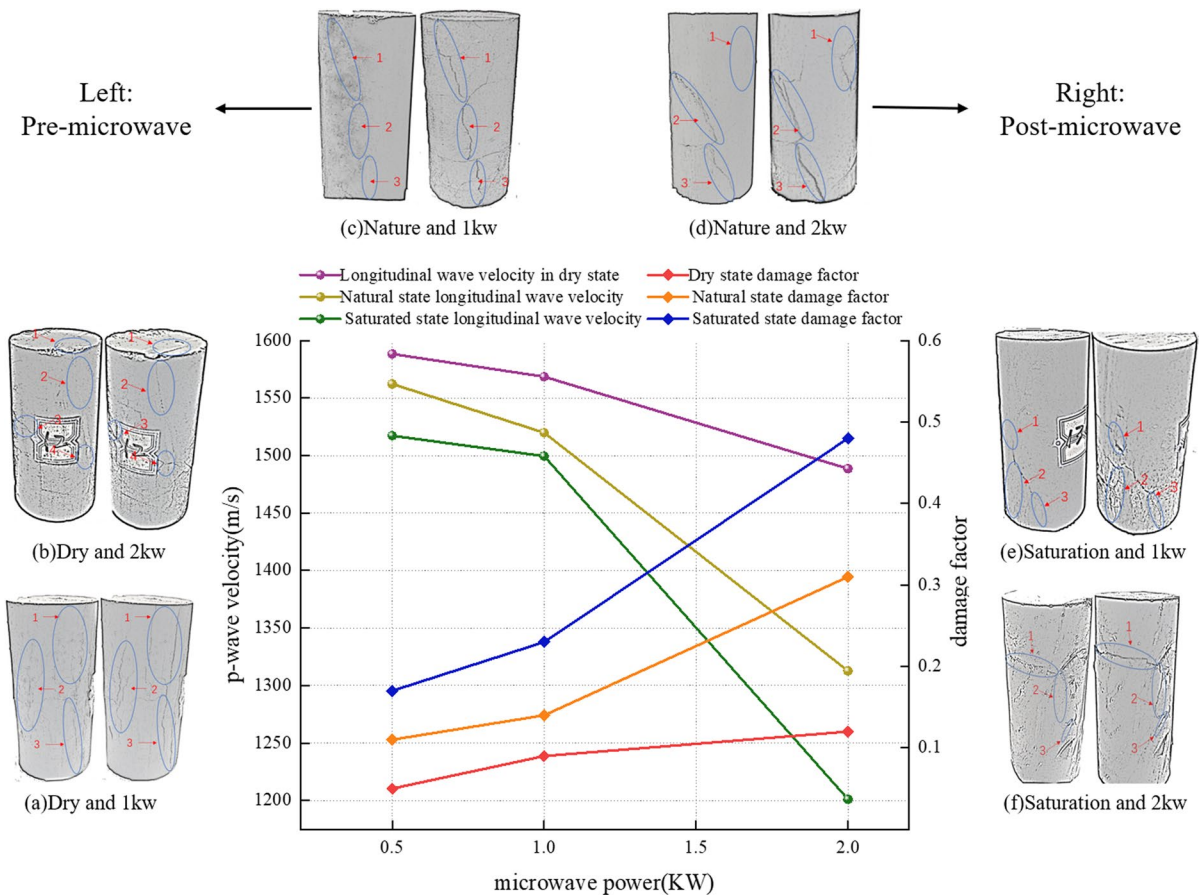


Fig. 5 Under the same microwave radiation time, the microwave power increases, the surface crack expansion of the coal sample and the internal relationship between the radiation power and the longitudinal wave velocity and the damage factor

3.1.2 Surface crack propagation law under microwave radiation

The proportion of tar and water in the components of coal samples is large, and the distribution is relatively discrete. The dielectric constants of these two substances are high. The specimens are heated in the microwave resonant cavity, and the temperature rises rapidly. Therefore, the temperature rise of the specimens is first local and then overall. At the same time, due to the discrete distribution of tar and water, the surface crack propagation of coal samples with different water saturation under microwave radiation is diverse.

During the experiment, the distribution of pore cracks on the surface of coal samples before and after microwave application under different water contents was obtained by photographing, and the images

obtained under microwave application under different water contents were summarized, classified, and processed. The results are as follows:

In the dry state, after the coal sample is irradiated by 1kw microwave, the hot spots are generated in the dense distribution area of tar and other high dielectric constant substances, and the thermal stress is continuously accumulated, resulting in micro-damage. The hot spots are continuously generated, and then the micro-fractures are developed and extended to the surface of the coal sample, and finally three vertical cracks are formed (marked 1,2,3 in Fig. 5a). After the coal sample with less initial damage is irradiated by 2kw microwave, the width and depth of the original crack increase, and the degree of damage increases. With the expansion and development of crack 1 (marked 1 in Fig. 5b), many small micro-cracks are generated around it. These micro-cracks intersect,

penetrate, and develop until the formation of macro-crack 2 (marked 2 in Fig. 5b). As the microwave radiation continues, the small cracks in the coal sample continue to develop and evolve, forming a new transverse crack (marked 4 in Fig. 5b).

Under the condition of natural water content, with the increase of water content, the surface failure point also increases, and the location of cracks on the surface of coal samples changes. The interaction between microwave and water improves the irradiation effect. The reason is that when the microwave is applied at the beginning, in a short time, the temperature increase of the specimen in the microwave resonator is low. When the temperature does not reach 100 °C, the free water of the coal sample volatilizes slowly. The water-free inside and on the surface of the specimen increases the dielectric constant of the specimen to some extent. On the other hand, the water molecule has a strong polarity. In the electromagnetic field, it swings rapidly with the high-frequency alternating electromagnetic field. In this process, a similar friction effect is generated, resulting in a large amount of heat. The generation of temperature gradient makes the primary cracks in some areas of the coal sample damaged by tension and gradually form macroscopic secondary cracks (labeled 1,2,3 in Fig. 5c). The degree of rupture of some holes and tiny cracks on

the surface of the coal sample continues to increase under the action of pyrolysis rupture, resulting in the formation of a certain amount of small cracks and holes, and finally forming new cracks (marked 1 in Fig. 5d).

In the saturated water state, the pyrolysis tar and minerals contained in the internal components of the coal sample are volatilized and removed in large quantities with the increase in temperature, resulting in a large number of pores. At the same time, some pores and micro-cracks on the surface of the coal sample continue to increase under the action of pyrolysis fracture, resulting in the formation of a certain amount of small crack holes, and finally converge to form new cracks (labels 1, 2, 3 in Fig. 5e). The cracks are interconnected and form a new crack network with the surrounding original cracks. Compared with the natural state, the fully saturated state causes the water in the pores and cracks of the coal sample to evaporate to produce a large vapor pressure, and the water vaporization impacts the primary cracks on the surface of the coal sample. The primary cracks are continuously widened under the action of the microwave and extend to the interior (Marks 1 and 3 in Fig. 5f). And, due to the vaporization of water, the temperature inside the cavity continues to rise, and with the pyrolysis loss of organic matter inside the

Table 4 Physical and mechanical properties of some coal samples in different states

Specimen number	Average compressive strength / MPa	Average peak strain	Average residual strain	Residual strength / Mpa	average elastic modulus/MPa	Elastic energy density / (mJ·m ⁻³)	dissipated energy density / (mJ·m ⁻³)
A _{1,2,3}	26.71	0.01734	0.01758	17.577	1173.9	0.17109	0.00555
B _{1,2,3}	20.41	0.01795	0.01856	0.739	793.78	0.12139	0.00662
C _{1,2,3}	14.84	0.02134	0.02184	0.602	545.99	0.12065	0.00615
D _{1,2,3}	12.2	0.02402	0.02588	11.308	345.46	0.08313	0.01697
E _{1,2,3}	8.51	0.0202	0.02069	0.116	296.39	0.05652	0.00386
F _{1,2,3}	3.91	0.02619	0.02815	3.181	102.86	0.03202	0.00647
G _{1,2,3}	13.32	0.02564	0.02762	10.789	519.5	0.09163	0.01732
G _{4,5,6}	13.16	0.02371	0.02513	9.475	555.04	0.08972	0.01655
G _{7,8,9}	11.91	0.02436	0.02614	10.599	488.92	0.08145	0.01782
H _{1,2,3}	9.13	0.02146	0.02302	4.166	425.44	0.06489	0.00571
H _{4,5,6}	8.69	0.02331	0.02501	0.217	372.8	0.06124	0.00642
H _{7,8,9}	7.93	0.02246	0.02437	2.116	353.07	0.05731	0.00463
I _{1,2,3}	4.63	0.02375	0.02516	4.16	188.73	0.03614	0.00746
I _{4,5,6}	4.12	0.02761	0.02881	3.91	149.22	0.03425	0.00548
I _{7,8,9}	3.78	0.02384	0.02576	3.22	155.46	0.02712	0.00568

coal sample, new cracks occur outside the specimen (label 2 in Fig. 5f).

3.2 Mechanical response characteristics

3.2.1 Strength softening characterization of coal samples under the interaction of microwave and water

Uniaxial, triaxial, and cyclic loading and unloading tests were carried out indoors to simulate the underground environment of coal samples under different water content conditions. It is of great significance to explore the deterioration trend and failure characteristics of mechanical properties of coal samples under different water content conditions (Shan et al. 2023; Gu et al. 2023).

The loading experiment of the press is carried out, and a series of physical and mechanical parameters are obtained. As shown in Table 4, the full stress–strain curve is drawn according to the axial displacement value and the stress of the coal sample specimen. According to the total input energy density, elastic energy density, and dissipated energy density, the change in energy density in the loading process is plotted.

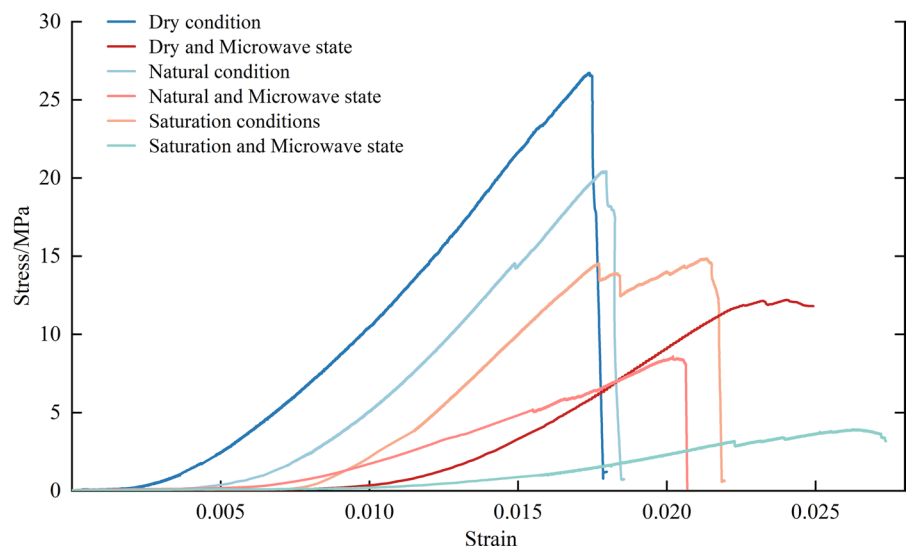
A uniaxial loading experiment was carried out to obtain the physical and mechanical parameters of coal samples under microwave and water content. The stress–strain curves of typical coal samples were drawn. The coal samples experienced four

stages: original compaction, linear elasticity, elastoplasticity, and final failure.

As shown in Fig. 6, under the condition of water content as a single variable, improving the water saturation of the specimen, the stress–strain curves of coal samples in different states show good similarity. The curve shows that the elastic energy density decreases, the total input energy decreases, and the peak stress decreases. Compared with dry coal samples, the peak strength of saturated coal samples decreases by about 45%. Can be concluded that, with the increase of moisture content of the coal sample specimen degradation phenomenon, the physical and mechanical parameters present coal sample specimen present a tendency of moves to the right compression stress–strain curve. Because coal samples are within primary cracks, due to the effect of "this moisture" of the water, under the microscopic makes original crack water molecules decreased in the internal cohesion of coal and rock particles Under the loading of the press, the cracks of the coal sample expand and deepen. At the macro level, the coal samples soften, the physical and mechanical parameters deteriorate, and the overall mechanical properties of the coal samples decrease.

Under the premise of water content as a known variable, microwave irradiation is introduced as another experimental variable. The experimental results show that with the introduction of microwave irradiation under different water content, In the dry state, the peak stress intensity decreased by about

Fig. 6 Stress–strain curves of tar-rich coal in different states



55.2%. The peak stress intensity in the natural state decreased by about 58.7%. In the saturated state, the peak stress intensity decreased most significantly, reaching 74.1%. It is further verified that the presence of water makes the effect of microwave radiation more significant.

To further analyze the strength softening degree of tar-rich coal under microwave and water degradation at the macro scale, the average peak strength in the experimental data is taken as the main parameter, and the corresponding strength softening coefficient is calculated by the following formula:

$$K_1 = \frac{R_i}{R_1} (i = 1, 2, 3) \tag{3}$$

$$K_2 = \frac{R_i}{R_4} (i = 4, 5, 6) \tag{4}$$

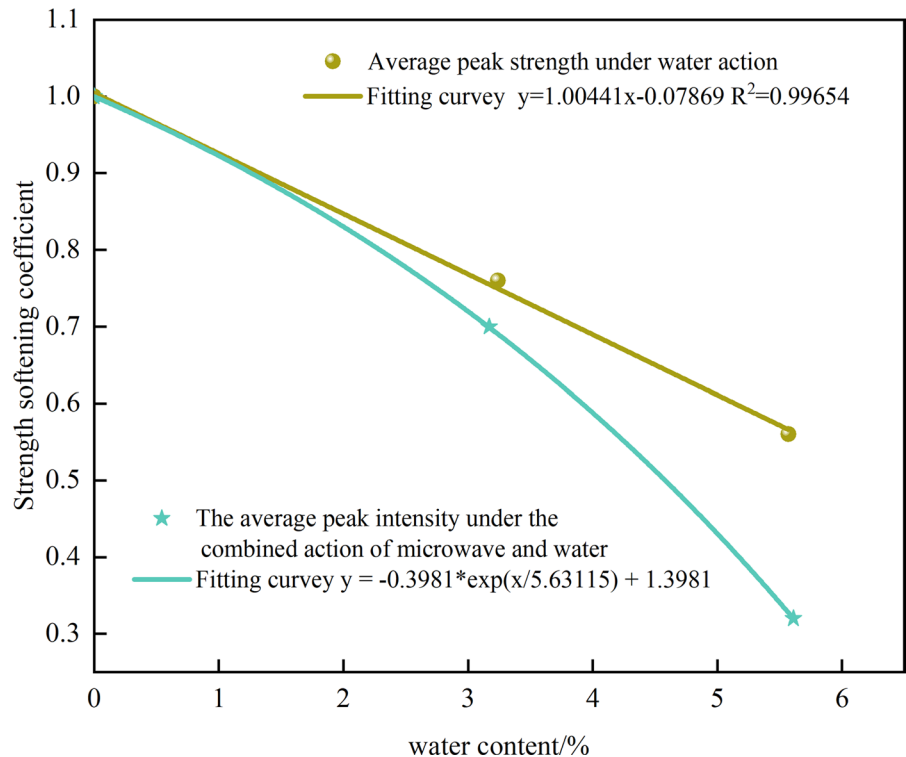
In the formula, K_1 is the strength softening coefficient of coal under the action of water, K_2 is the strength softening coefficient under microwave and water degradation, R_1 is the average peak strength under dry state, R_2 is the average peak strength under natural water content state, R_3 is the average peak strength under saturated water content state, R_4 is the average peak strength under dry state after microwave application, R_5 is the average peak strength under natural water content state after microwave application, R_6 is the average peak strength under saturated water content state after microwave application.

According to the data in Table 5, R_1 , R_2 , and R_3 are 26.71 MPa, 20.41 Mpa, and 14.84 MPa respectively, and R_4 , R_5 , and R_6 are 12.20 MPa, 8.51 Mpa, and 3.91 MPa respectively. In the condition of natural water, the strength attenuation value of the specimen reaches 0.76, and the strength softening coefficient

Table 5 Moisture content and peak strength of coal samples

Sample state	Average moisture content (%)	AVERAGE peak intensity (MPa)
Drying	0	26.71
Nature	3.24	20.41
Saturation	5.57	14.84
Drying and microwave	0	12.20
Nature and microwave	3.17	8.51
Saturated and microwave	5.61	3.91

Fig. 7 Characterisation of the softening factor of tar-rich coal strength in different states



under saturated water content is 0.56. The strength softening coefficient under natural water content after microwave application is 0.70, and the strength softening coefficient under saturated water content after microwave application is 0.32.

According to the above data, as shown in Fig. 7, the fitting relationship between the moisture content of coal samples and the strength softening coefficient is established. Through the fitting relationship, it can be concluded that compared with the effect of water alone, the strength degradation effect of coal samples under the combined action of microwave and water is more significant, the moisture content of the specimen is proportional to the degree of strength attenuation.

Taking dry coal samples as the main research object is conducive to establishing the strength-softening relationship between microwave power and various physical and mechanical parameters. By analyzing the changes of compressive strength, strain, and elastic modulus after loading by the press under different microwave radiation intensities, the average peak strength, average peak strain, and elastic modulus softening coefficient of dry coal samples under 0.5kw microwave radiation intensity are 0.50,0.68

and 0.44 respectively. Under 1kw microwave radiation intensity, the average peak strength, average peak strain, and elastic modulus softening coefficient of dry coal samples are 0.49, 0.73, and 0.47 respectively. Under 2kw microwave radiation intensity, the average peak strength, average peak strain, and elastic modulus softening coefficient of dry coal samples were 0.45, 0.71, and 0.42, respectively.

Comparing the experimental data and Fig. 8 Fitting results, it can be seen that the softening effect of coal samples under the combined action of microwave and water is better than that of microwave alone and water alone. At the same time, the changing trend of each physical and mechanical parameter is similar. The order of influence of microwave radiation on each parameter is peak strength>elastic modulus>peak strain.

3.2.2 Evolution law of energy density of coal samples

As shown in Fig. 9, due to the increase of water content, with the entry of water molecules between the particles of coal samples, the bonding force between the particles of the specimens decreases, and the

Fig. 8 The strength softening relationship between microwave power and physical and mechanical parameters

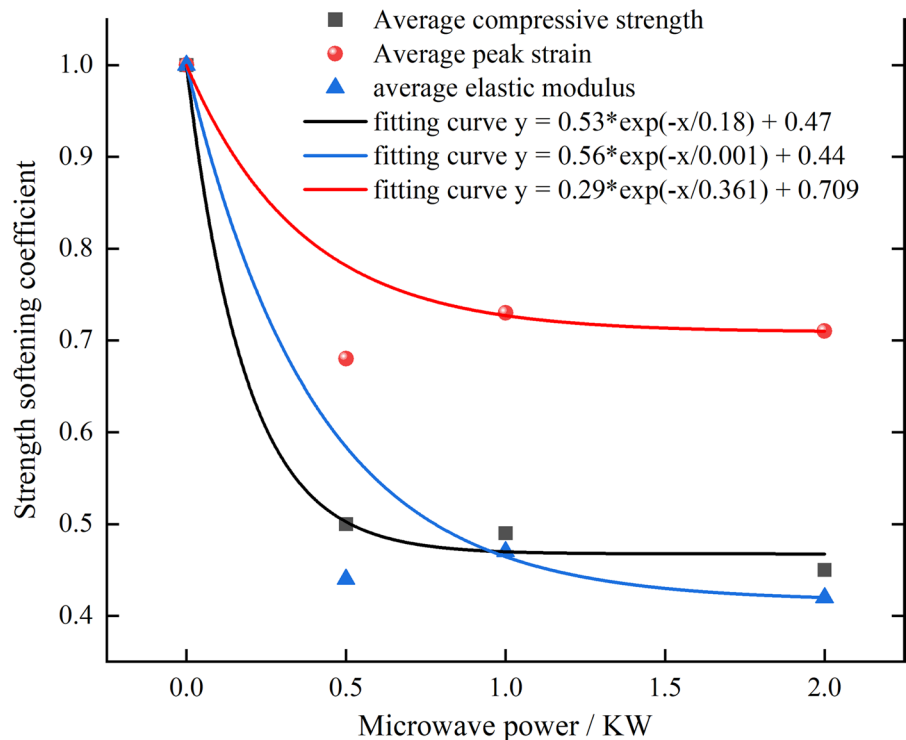
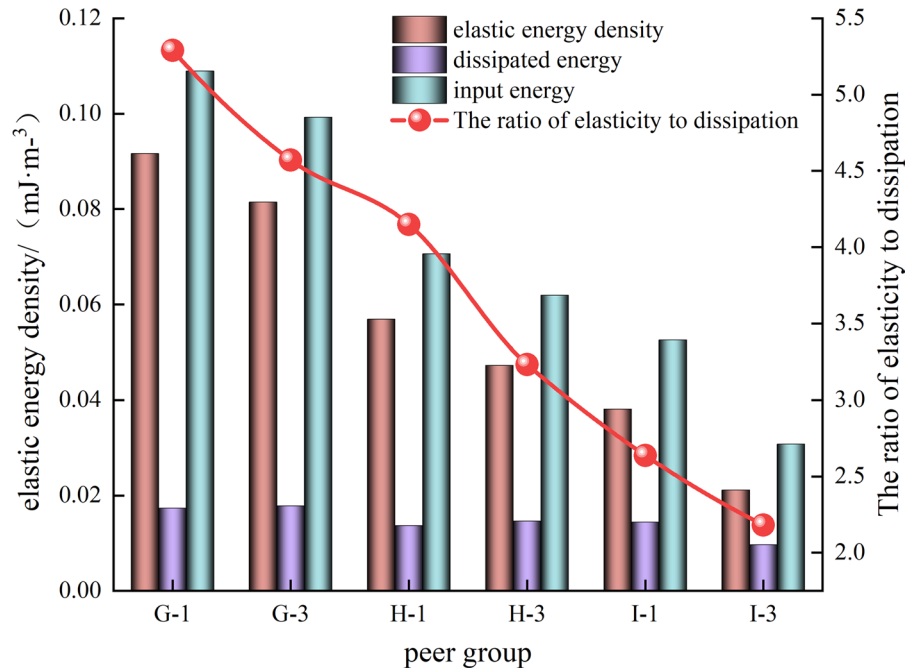


Fig. 9 Comparison of the energy density of tar-rich coal press before and after loading in different states



physical and mechanical parameters such as peak stress strength and elastic modulus deteriorate, and then the 'softening' phenomenon of coal samples occurs. The total input energy density and elastic energy density generally show a downward trend. When the energy density area continues to decrease, the dissipated energy density can remain relatively unchanged, or even slightly increase, and the dissipated energy density data is relatively high, indicating that during the loading process of the press, the coal sample still has high residual strength after compression failure. The ratio of the elastic energy density to the dissipated energy density can qualitatively describe whether the coal sample has an impact tendency. The larger the ratio, the smaller the energy density contained in the coal sample after the destruction. During the loading process of the coal sample, the energy is released in the form of kinetic energy, the coal sample collapses, and a rock burst occurs.

3.3 Study on fractal characteristics of coal samples under microwave radiation

3.3.1 Fractal characteristics of coal sample fragments

After microwave irradiation, cracks in the specimen gradually extend to the surface. The difference between the microwave radiation intensity and the moisture content of the coal sample will inevitably make the fracture network of the coal sample similar. However, limited to the maximum output power of the microwave resonant cavity, the coal sample only shows that with the increase of moisture content and microwave radiation power, fracture development is obvious, and fracture connectivity is greatly improved. To a certain extent, it is difficult to qualitatively express this 'similarity'. The water saturation of the coal sample increases, and there is very little initial damage inside the specimen. The microwave acts on the coal samples with different water saturation so that the number of secondary cracks increases continuously until the coal sample is distributed in the form of fragments after the press is loaded. In the process of evolution, the coal sample develops from micro-cracks to macro-cracks until the final fragment distribution and its structural evolution and physical

and mechanical parameters show extremely high self-similarity, that is, the fractal of coal sample fragments (Vishal and Chandra 2022). The fracture development of coal under microwave radiation is closely related to the distribution of fragments after loading by the press. Therefore, it is of great significance to explore the fractal characteristics of fragments of water-bearing coal samples loaded by the press after microwave radiation.

In this study, the differences in mass and size of broken blocks of coal samples with different moisture contents under microwave radiation were statistically analyzed, and the influence of different external conditions on the distribution of broken blocks of coal samples was quantitatively analyzed.

The equivalent side length-coal sample debris (block) is used to calculate the fractal dimension. According to the interval classification method, and combined with the actual situation, the coal sample

debris is divided into three groups according to the equivalent side length, which is particles (<5 mm), medium particles (<30 mm), and coarse particles (<60 mm). The difference in debris (block) quality under different equivalent side lengths is studied. After loading by the press, the coal sample is crushed to produce a large number of particles. To further study the distribution characteristics of coal sample fragments, the above particle intervals are redivided, and the coal sample fragments (chips) with a size of less than 5.0 mm are redivided into four small intervals. Due to the large number, it is not easy to measure, and the molecular sieve with the corresponding aperture is used for screening. For coal samples with a size greater than 5.0 mm, the number of fragments is relatively small. The maximum size of the fragments can be measured by a vernier caliper, and then the weight can be recorded according to the classification of the particle size range of the fragments. The classification criteria and analysis methods of coal sample fragments are shown in Table 6 below.

According to the data in Table 7 and Fig. 10, it can be seen that with the increase in water content, the proportion of coal sample fragments in the particle group gradually decreases, and the mass proportion of 0–0.5 mm decreases from 4.72 to 0.6%. After microwave treatment, due to the increase in microwave power, the transformation effect on the internal structure of coal samples is enhanced, and the physical and mechanical properties are degraded. After the introduction of the microwave, the overall trend of the mass percentage of medium-grained and coarse-grained coal samples significantly improved.

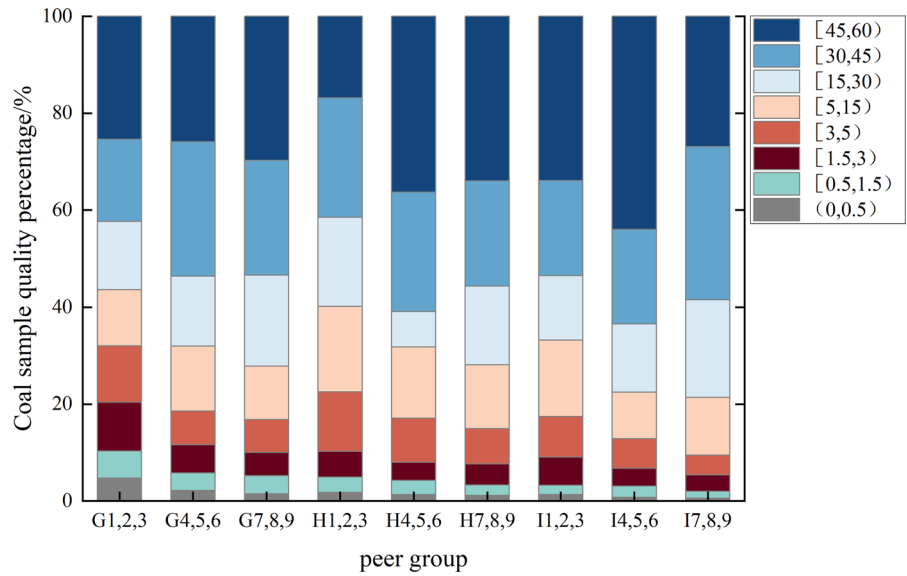
Table 6 Coal classification standard and analysis method

Fragment category	Particle size range /mm	Research method
Particle	(0, 0.5)	Screening method mass weighing
	[0.5, 1.5)	
	[1.5, 3)	
	[3, 5)	
Medium grain	[5, 15) [15, 30)	Mass weighing
Coarse grain	[30, 45) [45, 60)	Mass weighing

Table 7 Distribution interval and mass percentage of coal fragments

Dimension/ mm	Coal sample quality percentage under different conditions/%								
	Drying and 0.5 kw	Drying and 1 kw	Drying and 2 kw	Nature and 0.5 kw	Nature and 1 kw	Nature and 2 kw	Saturation and 0.5 kw	Saturation and 1 kw	Saturation and 2 kw
(0, 0.5)	4.72	2.15	1.5	1.74	1.34	1.13	1.3	0.76	0.6
[0.5, 1.5)	5.59	3.61	3.72	3.22	2.89	2.17	1.96	2.33	1.4
[1.5, 3)	10.04	5.82	4.79	5.31	3.76	4.35	5.8	3.67	3.36
[3, 5)	11.66	6.97	6.78	12.28	9.13	7.31	8.38	6.07	4.1
[5, 15)	11.54	13.42	11.02	17.62	14.66	13.17	15.77	9.6	11.93
[15, 30)	14.11	14.33	18.75	18.31	7.32	16.19	13.24	14.06	20.1
[30, 45)	16.95	27.77	23.64	24.66	24.58	21.7	19.58	19.49	31.57
[45, 60)	25.36	25.88	29.75	16.85	36.31	33.96	33.93	43.92	26.89

Fig. 10 Distribution interval and mass percentage of coal fragments



The mass percentage of coarse-grained coal samples is the highest, from 42.31 to 58.46%, with an increase of 16.15%. Is the introduction of microwave radiation and an increase in the moisture content, the particle group of coal sample fragments gradually decreases, the grain and coarse grain size range of coal sample fragments gradually increases, and coal sample broken block distribution by large size and small size range gradually to the middle size.

3.3.2 Effect of microwave radiation on the fractal dimension of coal samples with different moisture content

The G-G-S distribution function is authoritative in deducing the fractal characteristics of coal samples (Lai et al. 2023).

The G-G-S distribution function is expressed as follows:

$$y = \left(\frac{r}{r_m}\right)^\alpha \tag{5}$$

where m is the mass distribution parameter of the coal sample, r is the maximum particle size of fragments, and α is the block distribution parameter of the coal sample.

At the same time, $m(r)$ is the mass of the fragments under the screen statistics when the equivalent

particle size is less than the characteristic size r , and M is the total mass of the coal sample.

Therefore, the above formula can be converted to:

$$\frac{m(r)}{M} = \left(\frac{r}{r_m}\right)^\alpha \tag{6}$$

Derivation of the above formula can be obtained:

$$dm \propto r^{\alpha-1} dr \tag{7}$$

The relationship between the quantity and mass increment of coal sample fragments:

$$dm \propto r^3 dN \tag{8}$$

The relationship between the fractal dimension D , the characteristic size r , and the number of equivalent particle size fragment N of coal sample crushing are:

$$N \propto r - D \tag{9}$$

By combining the above formulas, it can be concluded that:

$$\alpha = \frac{\lg(M(r)/M)}{\lg r} \tag{10}$$

$$D = 3 - \alpha \tag{11}$$

A is the slope value in the double logarithmic coordinates of $\lg r - \lg M(r)/M$; r is the equivalent side length (the maximum value of the size

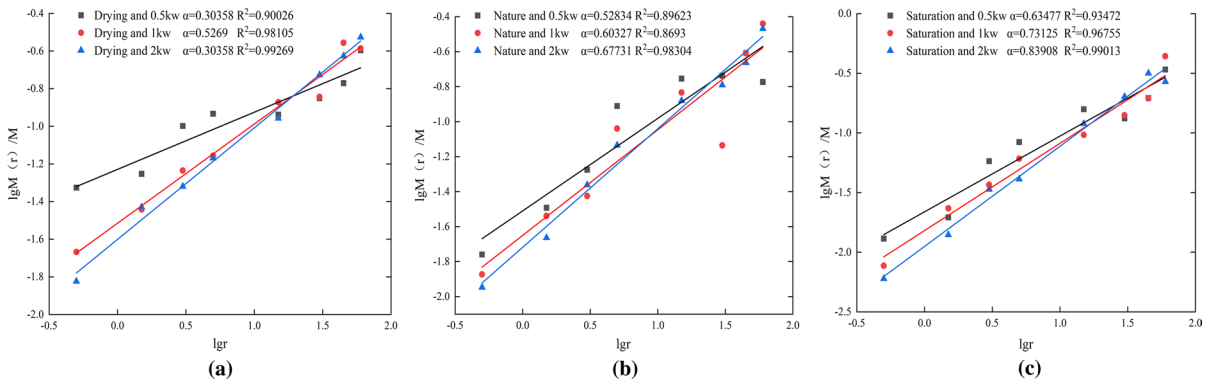


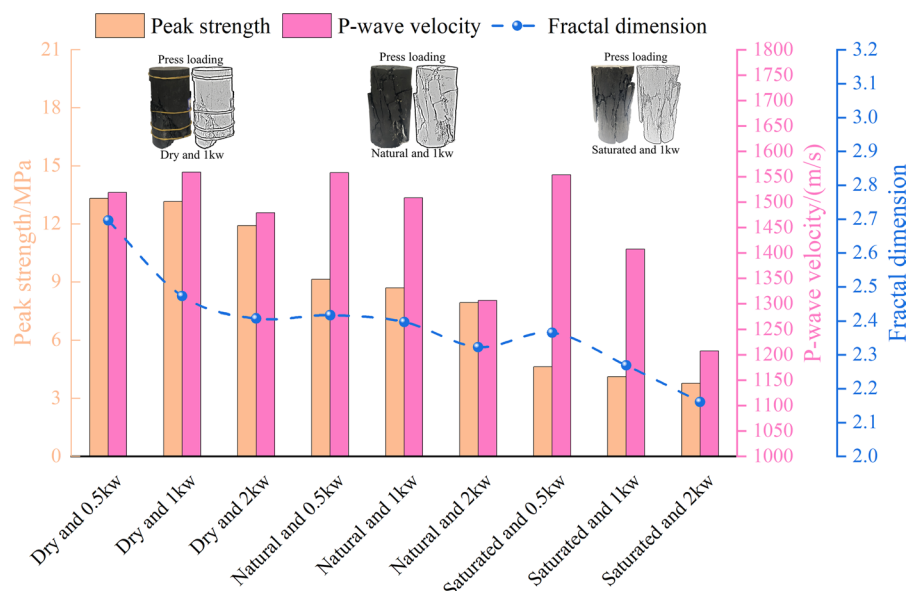
Fig. 11 Double logarithmic curve of equivalent side length-mass distribution of coal samples in different states; **a** Drying and Microwave; **b** Nature and microwave; **c** Saturation and Microwave

corresponding to the interval); $m(r)$ is the mass of coal sample fragments under the equivalent side length r ; m is the total mass of debris (block) in the calculation scale of coal sample; d is the fractal dimension.

As shown in Fig. 11, in the drying state, the microwave power was increased from 0.5kw to 2kw, and the fractal dimensions of coal samples were 2.696, 2.473, and 2.407, respectively. Under the condition of natural water content, the microwave power is increased from 0.5 to 2 kw, and the fractal dimensions of coal sample fragments are 2.471, 2.397, and 2.323, respectively. Under the

condition of saturated water content, the microwave power is increased from 0.5 to 2 kw, and the fractal dimensions of coal sample fragments are 2.365, 2.269 and 2.161, respectively. Under the combined action of microwave and water, the fractal dimension decreases obviously. With the increase of water content, the fractal dimension of coal samples decreases linearly after the introduction of microwave. Judging from the decreasing trend of fractal dimension, the influence of microwave power on fractal dimension is stronger than that of water content. Overall, under the combined action of microwave and water, the fractal dimension decreases

Fig. 12 Under the interaction of microwave and water, the relationship between fractal dimension, compressive strength, and longitudinal wave velocity of coal samples



significantly, and both of them promote the decrease of the fractal dimension.

Both water and microwave radiation intensity can degrade coal samples, and the difference in water content of coal samples and applied microwave radiation power will inevitably make the loading results of the press appear in the form of coal sample fragments. The higher the degree of coal fragmentation, the larger the fractal dimension, and the fractal dimension can characterize the effect of microwave radiation. The longitudinal wave velocity is mainly affected by the development of internal cracks in coal specimens. The denser the specimen is, the greater the wave velocity is. On the contrary, the more developed the internal cracks in the specimen are, the smaller the wave velocity is. At the same time, the lower the peak intensity, the more significant the microwave radiation effect. Figure 12 shows the relationship between microwave radiation power and fractal dimension, longitudinal wave velocity, and peak intensity under different water content conditions. The results show that the fractal dimension is inversely proportional to the water content and the microwave radiation intensity, and the fractal dimension is positively correlated with the peak intensity and the longitudinal wave velocity.

4 Discussion

According to the experimental results, the microwave radiation effect of oil-rich coal under different water saturation was compared. The longitudinal wave velocity of water-saturated coal samples decreased obviously, and the microstructure development of coal samples such as pores and cracks was obvious. According to the microcosmic principle of microwave radiation, coal particles are a kind of dielectric, and the presence of water improves the dielectric constant of coal samples. The existing polar molecules of the coal sample, the newly formed polar molecules of the coal sample, and the water are rearranged under the action of field force and constantly change their positions with the high-frequency alternating electromagnetic field. In the change of position, the molecular motion should overcome the interference and obstruction between the original thermal motion, and produce a friction-like effect, to increase the temperature

of coal. According to the macroscopic principle of microwave radiation, under the condition of microwave field heating of a water-saturated coal sample, on the one hand, the water in the original pores and cracks in the interior vaporizes and produces water vapor. Vapor pressure is generated and acts on the pores and cracks in the coal sample, forming an effect similar to splitting and stretching, which further expands the pores and cracks. On the other hand, because the water on the surface of the coal sample is in the microwave field environment, evaporation generates water vapor, which further increases the temperature in the microwave field and promotes the breeding and expansion of the coal rock microstructure. Therefore, water in coal samples under microwave radiation is conducive to the development of microfissure structures and the deterioration of the physical and mechanical properties of coal samples.

Microwave can crack tar-rich coal. When the water content increases, the cracking effect is further enhanced. The internal reason lies in the characteristics of microwave and tar-rich coal:

Microwave penetration is strong, and the microwave is radiated into the heated coal sample. The microwave can directly penetrate the coal sample so that the polarized molecules in the sample constantly rearrange and change direction with the change of alternating electromagnetic field and promote their violent movement. In this process, the polarized molecules rub against each other, collide with each other, produce heat and increase temperature. Because the warming process is completed synchronously for the whole sample, it has overall warming and fast warming, which is an efficient warming method.

Due to the selective heating of microwave, the material components with a high dielectric constant in tar-rich coal preferentially absorb heat, resulting in temperature differences in some areas of the coal sample, and then forming a temperature gradient. The generation of temperature gradient makes a certain amount of thermal stress act on the inside of the coal sample. When the thermal stress is greater than the strength of the coal sample (mostly tensile strength, rock compressive not tensile), small cracks are generated, small cracks are developed and penetrated, and finally macroscopic cracks are formed on the surface of the coal sample.

Tar-rich coal contains a large amount of organic matter, which makes it significantly different from the

failure mode, failure mode, generation, and expansion of failure points of inorganic rocks. During microwave heating, organic matter is pyrolyzed with an increase in temperature. The escape of pyrolysis products greatly changes the internal structure of coal samples. The decomposition of organic matter causes a large number of pores in coal samples. The solid skeleton of coal samples changes significantly, and the physical and mechanical parameters deteriorate obviously.

Accordingly, the main reasons for the destruction of tar-rich coal are the pyrolysis fracture of coal caused by rich organic matter, the thermal stress damage caused by the selective heating of coal samples by microwave radiation, and the splitting tensile transformation of coal samples by steam pressure formed by water evaporation under the condition of the large water content of coal samples.

This study provides a new scheme for the weakening of coal mine roof: in the early stage, the hydraulic fracturing hole and microwave irradiation port were drilled by a drilling rig, and the microwave irradiation was carried out by microwave radiation equipment (microwave radiation power $\geq 15\text{kw}$). The specific microwave power and microwave radiation time were preliminarily determined by the specific working conditions under different lithologies and different water saturation. Then, the borehole peeping and ultrasonic testing equipment were used to explore the crack formation and the loosening range of the rock after microwave irradiation, and then the microwave power, microwave irradiation time, and the borehole spacing between the hydraulic fracturing hole and microwave irradiation hole were finally determined.

5 Conclusion

1. After microwave irradiation of water and tar with high content of tar-rich coal components, due to pyrolysis, the internal micro-crack structure of coal samples develops, and the pores and cracks increase. Under the same microwave radiation condition, with the increase of water saturation, the longitudinal wave velocity and peak intensity decrease.
2. After microwave radiation, the uniaxial compression results show that the coal sample is damaged

by load, there is still a high residual strength, the ratio of elastic energy to dissipation energy decreases, and the possibility of rockburst of the coal sample decreases. The strength softening degree of coal specimen under the degradation of microwave and water is the highest, followed by microwave and water.

3. The fractal dimension is inversely proportional to the moisture content and microwave radiation intensity, and the fractal dimension has a significant positive correlation with the peak intensity and longitudinal wave velocity.

Author contributions PY: Performed the experiments; Analyzed and interpreted the data; Wrote the paper. PS: Conceived and designed the experiments; Performed the experiments. HX: Performed the experiments. JC: Performed the experiments. ZL: Analyzed and interpreted the data. HS: Analyzed and interpreted the data; Wrote the paper.

Funding We thank the National Natural Science Foundation of China (52274138, 51904227), the Innovation Capability Support Program of Shaanxi (2022KJXX-58), and the Yulin High-tech Zone Science and Technology Plan Project (ZD-2021-01) for its support of this study. We thank the academic editors and anonymous reviewers for their kind suggestions and valuable comments.

Availability of data and materials The authors confirm they have included a data availability statement in their main manuscript file. The datasets generated during and/or analyzed during the current study are available from the corresponding author upon reasonable request.

Declarations

Ethics approval and consent to participate The authors declare that the submitted work is original and has not been submitted to more than one journal for simultaneous consideration.

Consent to publish The authors agree to publication in the Geomechanics and Geophysics for Geo-Energy and Geo-Resources and also to publication of the article in English Springer in Springer's corresponding English-language journal.

Competing interests The authors declare that they have no competing interests.

Open Access This article is licensed under a Creative Commons Attribution 4.0 International License, which permits use, sharing, adaptation, distribution and reproduction in any medium or format, as long as you give appropriate credit to the original author(s) and the source, provide a link to the Creative Commons licence, and indicate if changes were made. The

images or other third party material in this article are included in the article's Creative Commons licence, unless indicated otherwise in a credit line to the material. If material is not included in the article's Creative Commons licence and your intended use is not permitted by statutory regulation or exceeds the permitted use, you will need to obtain permission directly from the copyright holder. To view a copy of this licence, visit <http://creativecommons.org/licenses/by/4.0/>.

References

- Bai GG, Sun Q, Jia HL, Ge ZL, Li PF (2021) Variations in fracture toughness of SCB granite influenced by microwave heating. *Eng Fract Mech* 258:108048. <https://doi.org/10.1016/j.engfracmech.2021.108048>
- Deyab SM, Rafezi H, Hassani F, Kermani M, Sasmito AP (2020) Experimental investigation on the effects of microwave irradiation on kimberlite and granite rocks. *J Rock Mech Geotech Eng* 13(2):267–274. <https://doi.org/10.1016/j.jrmge.2020.09.001>
- Ellison C, Abdelsayed V, Smith M, Shekhawat D (2022) Comparative evaluation of microwave and conventional gasification of different coal types: experimental reaction studies. *Fuel* 321:124055. <https://doi.org/10.1016/j.fuel.2022.124055>
- Feng XT, Zhang JY, Yang CX, Tian J, Lin F, Li SP, Su XX (2021) A novel true triaxial test system for microwave-induced fracturing of hard rocks. *J Rock Mech Geotech Eng* 13(5):961–971. <https://doi.org/10.1016/j.jrmge.2021.03.008>
- Gautam PK, Verma AK, Jha MK, Sarkar K, Singh TN, Bajpai RK (2016) Study of strain rate and thermal damage of Dholpur sandstone at elevated temperature. *Rock Mech Rock Eng* 49(9):3805–3815. <https://doi.org/10.1007/s00603-016-0965-5>
- Ge ZL, Sun Q (2021) Acoustic emission characteristics of gabbro after microwave heating. *Int J Rock Mech Min Sci* 138:104616. <https://doi.org/10.1016/j.ijrmms.2021.104616>
- Gu HL, Lai XP, Tao M, Cao WZ, Yang ZK (2023) The role of porosity in the dynamic disturbance resistance of water-saturated coal. *Int J Rock Mech Min Sci* 166:105388. <https://doi.org/10.1016/j.ijrmms.2023.105388>
- Gu HL, Lai XP, Tao M, Momeni A, Zhang QL (2023) Dynamic mechanical mechanism and optimization approach of roadway surrounding coal water infusion for dynamic disaster prevention. *Measurement* 223:113639. <https://doi.org/10.1016/j.measurement.2023.113639>
- Hong YD, Lin BQ, Zhu CJ, Wang Z, Liu JQ, Saffari P, Nie W (2020) Image and ultrasonic analysis-based investigation of coal core fracturing by microwave energy. *Int J Rock Mech Min Sci* 127:104232. <https://doi.org/10.1016/j.ijrmms.2020.104232>
- Hu GZ, Yang N, Zhu J, Qin W, Huang JX (2020) Evolution characteristics of microwave irradiation on permeability and surface cracks of coal with water: an experimental study. *J China Coal Soc* 45(S2):813–822. <https://doi.org/10.13225/j.cnki.jccs.2020.0148>
- Hu GZ, Wang CB, Xu JL, Wu XF, Qin W (2021) Experimental investigation on decreasing burst tendency of hard coal using microwave irradiation. *J China Coal Soc* 46(2):450–465. <https://doi.org/10.13225/j.cnki.jccs.XR20.1906>
- Ju Y, Zhu Y, Zhou HW, Ge SR, Xie HP (2021) Microwave pyrolysis and its applications to the in situ recovery and conversion of oil from tar-rich coal: an overview on fundamentals, methods, and challenges. *Energy Rep* 7:523–536. <https://doi.org/10.1016/j.egy.2021.01.021>
- Kahraman S, Canpolat AN, Fener M, Kilic CO (2020) The assessment of the factors affecting the microwave heating of magmatic rocks. *Geomech Geophys Geo* 6(4):1–16. <https://doi.org/10.1007/s40948-020-00197-3>
- Khadijeh M, Yehya A, Maalouf E (2022) Propagation and geometry of multi-stage hydraulic fractures in anisotropic shales. *Geomech Geophys Geo* 8(4):124. <https://doi.org/10.1007/s40948-022-00425-y>
- Lai YM, Zhao K, He ZW, Yu X, Yan YJ, Li Q, Shao H, Zhang XW, Zhou Y (2023) Fractal characteristics of rocks and mesoscopic fractures at different loading rates. *Geomech Energy Envir* 33:100431. <https://doi.org/10.1016/j.gete.2022.100431>
- Li H, Lin BQ, Hong YD, Yang W, Liu T, Huang ZB, Wang R (2017) Effect of microwave irradiation on pore and fracture evolutions of coal. *J China U Min Techno* 46(6):1194–1201. <https://doi.org/10.13247/j.cnki.jcmt.000754>
- Li H, Tian L, Huang BX, Lu JX, Shi SL, Lu Y, Huang F, Liu Y, Zhu XN (2020) Experimental study on coal damage subjected to microwave heating. *Rock Mech Rock Eng* 53(12):5631–5640. <https://doi.org/10.1007/s00603-020-02230-z>
- Lin DN, Chen SR (2005) Experimental study on damage evolution law of rock under cyclical impact loadings. *Chin J Rock Mech Eng* 22:4094–4098. <https://doi.org/10.3321/j.issn:1000-6915.2005.22.014>
- Liu J, Xue Y, Zhang Q, Shi F, Wang HM, Liang X, Wang SH (2022) Investigation of microwave-induced cracking behavior of shale matrix by a novel phase-field method. *Eng Fract Mech* 271:108665. <https://doi.org/10.1016/j.engfracmech.2022.108665>
- Lu J, Xie HP, Li MH, Li CB, Gao MZ, Shang DL, Li JH (2022) Effect of microwave radiation on mechanical behaviors of tight fine sandstone subjected to true triaxial stress. *Int J Rock Mech Min Sci* 152:105063. <https://doi.org/10.1016/j.ijrmms.2022.105063>
- Luo Y, Xu K, Huang JH, Li XP, Liu TT, Qu DX, Chen PP (2021) Impact analysis of pressure-relief blasting on roadway stability in a deep mining area under high stress. *Tunn Undergr Space Technol* 110:103781. <https://doi.org/10.1016/j.tust.2020.103781>
- Ma ZJ, Zheng YL, Li JC, Zhao XB, Zhao QH, He JL, Fu HY (2022) Characterizing thermal damage of diorite treated by an open-ended microwave antenna. *Int J Rock Mech Min Sci* 149:104996. <https://doi.org/10.1016/j.ijrmms.2021.104996>
- Mushtaq F, Mat R, Ani FN (2014) A review on microwave assisted pyrolysis of coal and biomass for fuel production.

- Renew Sust Energy Rev 39:555–574. <https://doi.org/10.1016/j.rser.2014.07.073>
- Nicco M, Holley EA, Hartlieb P, Pfaff K (2020) Textural and mineralogical controls on microwave-induced cracking in granites. *Rock Mech Rock Eng* 53(10):4745–4765. <https://doi.org/10.1007/s00603-020-02189-x>
- Shan PF, Li W, Lai XP, Zhang S, Chen XZ, Wu XC (2023) Research on the response mechanism of coal rock mass under stress and pressure. *Materials* 16(8):3235. <https://doi.org/10.3390/ma16083235>
- Shi QM, Li CH, Wang SM, Ji RJ, Xue WF, Mi YC, Wang SQ, Cai Y (2023) Variation of molecular structures affecting tar yield: a comprehensive analysis on coal ranks and depositional environments. *Fuel* 335:127050. <https://doi.org/10.1016/j.fuel.2022.127050>
- Tripathi A, Gupta N, Singh AK, Mohanty SP, Rai N, Pain A (2021) Effects of elevated temperatures on the microstructural, physico-mechanical and elastic properties of Barakar sandstone: a study from one of the world's largest underground coalmine fire region, Jharia, India. *Rock Mech Rock Eng* 54(3):1293–1314. <https://doi.org/10.1007/s00603-020-02315-9>
- Vishal V, Chandra D (2022) Mechanical response and strain localization in coal under uniaxial loading, using digital volume correlation on X-ray tomography images. *Int J Rock Mech Min Sci* 154:105103. <https://doi.org/10.1016/j.ijrmms.2022.105103>
- Xu HC, Lai XP, Shan PF, Yang YB, Zhang S, Yan BX, Zhang Y, Zhang N (2023) Energy dissipation characteristics and shock mechanism of coal-rock mass induced in steeply-inclined mining: comparison based on physical simulation and numerical calculation. *Acta Geotech* 18(2):843–864. <https://doi.org/10.1007/s11440-022-01617-2>
- Yang N, Hu GZ, Qin W, Huang JX (2021) Experimental study on mineral variation in coal under microwave irradiation and its influence on coal microstructure. *J Nat Gas Sci Eng* 96:104303. <https://doi.org/10.1016/j.jngse.2021.104303>
- Zhang Y, Cao SG, Zhang N, Zhao CZ (2020) The application of short-wall block back fill mining to preserve surface water resources in Northwest China. *J Clean Prod* 261:121232. <https://doi.org/10.1016/j.jclepro.2020.121232>
- Zhang GC, He FL, Lai YH, Song JW, Xiao P (2016) Reasonable width and control technique of segment coal pillar with high-intensity fully-mechanized caving mining. *J China Coal Soc* 41(9):2188–2194. <https://doi.org/10.13225/j.cnki.jccs.2016.0145>
- Zhang SC, Li YY, Shen BT, Sun XZ, Gao LQ (2019) Effective evaluation of pressure relief drilling for reducing rock bursts and its application in underground coal mines. *Int J Rock Mech Min Sci* 114:7–16. <https://doi.org/10.1016/j.ijrmms.2018.12.010>
- Zhang JY, Feng XT, Yang CX, Lin F, Li SP, Tong TY, Su XX (2022) The characteristics and mechanism of microwave-induced borehole fracturing of hard rock under true triaxial stress. *Eng Geol* 306:106768. <https://doi.org/10.1016/j.enggeo.2022.106768>
- Zhang Y, Liu YZ, Lai XP, Cao SG, Yang YB, Yan BX, Bai LC, Tong L, He W (2023) Transport mechanism and control technology of heavy metal ions in gangue backfill materials in short-wall block backfill mining. *Sci Total Environ* 895:165139. <https://doi.org/10.1016/j.scitotenv.2023.165139>
- Zhao HB, Wang ZW, Zhang H, Li W (2016) Effects of dynamic loads on development of internal microstructure and distribution of new surface fractures of coal. *Chin J Rock Mech Eng* 35(5):971–979. <https://doi.org/10.13722/j.cnki.jrme.2015.1541>
- Zhao QH, Zhao XB, Zheng YL, Li JC, He L, Zou CJ (2020) Microwave fracturing of water-bearing sandstones: heating characteristics and bursting. *Int J Rock Mech Min Sci* 136:104495. <https://doi.org/10.1016/j.ijrmms.2020.104495>

Publisher's Note Springer Nature remains neutral with regard to jurisdictional claims in published maps and institutional affiliations.